

In:

Fluid Inclusions in Minerals: Methods and Applications

Edited by Benedetto De Vivo & Maria Luce Frezzotti

**Short Course of the Working Group (IMA)
„Inclusions in Minerals“
(Pontignano – Siena, 1-4 September 1994)**

Application of clathrates to fluid inclusion studies

Ronald J. Bakker and Régis Thiéry

Page 191 – 208.

Application of clathrates to fluid inclusion studies

Ronald J. Bakker & Régis Thiéry

Centre de Recherches sur la Géologie des Matières Primaires Minérales et énergétiques (CREGU), B.P. 23, F-54501, Vandoeuvre-lès-Nancy (France).

Abstract

Semi-qualitative isobaric and isothermal phase diagrams are presented, which describe phase transitions involving clathrates in the $\text{H}_2\text{O}-\text{CO}_2$, $\text{H}_2\text{O}-\text{CH}_4$ and the $\text{H}_2\text{O}-\text{CO}_2-\text{NaCl}$ fluid system. For quantitative analysis, a model based on statistical thermodynamics is introduced to predict clathrate stability conditions in the presence of fluids within these systems. The phase diagrams can be used to deduce phase transitions in fluid inclusions, i.e. isochorical systems, during heating and freezing cycles at microthermometric stages, as illustrated with several examples.

Introduction

Fluid inclusions which contain a mixture of H_2O , gases, and occasionally salts form an ice-like solid phase close to the freezing point of pure H_2O . This solid phase which is called clathrate or gas hydrate can be visually distinguished from pure ice in fluid inclusions (Fig.1). The formation of the clathrate phase complicates the interpretation of low temperature microthermometric measurements, as it consumes both H_2O and gases. Any remaining aqueous solution phase will be more saline because salt is excluded from the clathrate phase, and any remaining volatile-rich phase will be less dense. Thus, in the presence of a clathrate it is not possible to derive the salinity directly from the melting temperature of pure ice (Potter and Brown, 1977; Bodnar, 1983), and in multi-component salt-free systems it is not possible to derive directly the density and molar volume of the $\text{CO}_2-\text{CH}_4-\text{N}_2$ -rich phase from liquid-vapour transitions (Kerkhof, 1990; Thiéry et al, 1994).

Determination of P-T-V-X properties of phase transitions involving clathrates is necessary to improve the compositional and volumetric characterisation of the fluid in individual inclusions. First, a few words will be given about the general chemistry and structure of clathrates, and a short outline is given about the stability model. Then, the topology of $\text{H}_2\text{O}-\text{CO}_2$, $\text{H}_2\text{O}-\text{CH}_4$ and $\text{H}_2\text{O}-\text{CO}_2-\text{NaCl}$ systems are described. Finally, some examples are given of phase transitions involving clathrates within fluid inclusions during heating. This course should be viewed as an application of concepts which have been presented elsewhere (e.g. Dubessy et al., 1992; Diamond, 1992 and 1994), and as an introduction to more applied papers about the interpretation of clathrate equilibria in fluid inclusions.

Chemistry and structure of clathrates

A clathrate has a metastable framework of H_2O molecules with various types of cavities, which is stabilised by the presence of gas molecules in part of these cavities (Stackelberg and Müller, 1954; Waals and Platteeuw, 1959; Sloan, 1990). Clathrates crystallise in at least two possible

cubic structures, usually referred to as *Structure I* and *Structure II* (Fig.2). H₂O molecules are linked to each other by H-bonds, similar to ice, whereas encaged gas molecules interact only with their neighbouring H₂O molecules by weak physical forces, which are the sum of repulsive and attractive forces (e.g. Prausnitz et al., 1986).

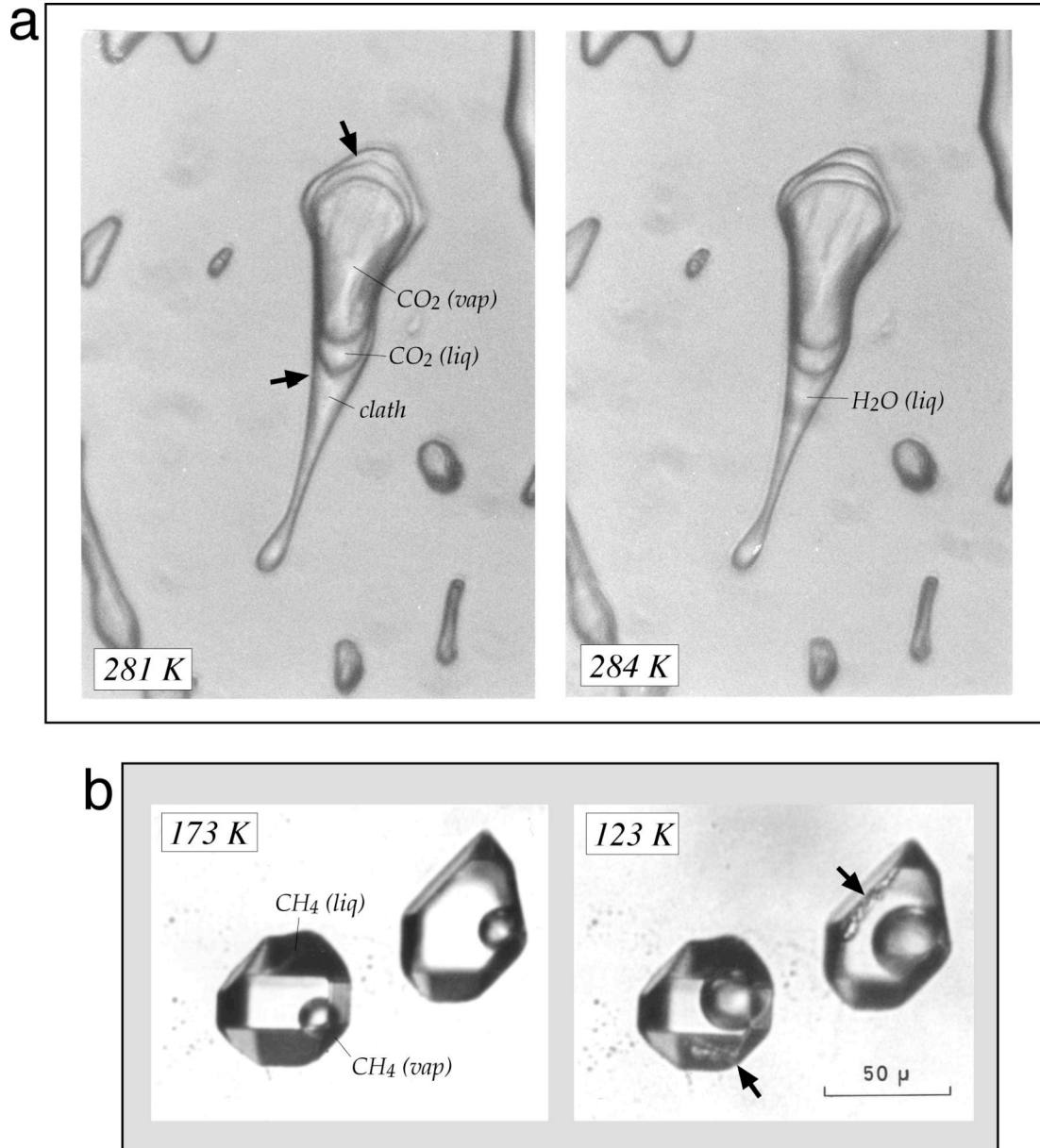


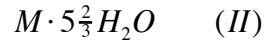
Fig.1.

a. Melting of clathrate in a H₂O-CO₂-rich synthetic fluid inclusion during a heating run at Q2 conditions. The inclusion contains 20 mole% CO₂. At 281 K, the presence of a solid clathrate phase is evident by the irregular meniscus between the outer phases (arrows). This meniscus is smoothly curved at 284 K, indicating the presence of a H₂O-rich liquid phase wetting the inclusion walls .

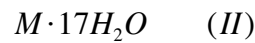
b. An apparent two phase, i.e. liquid and vapour CH₄, natural fluid inclusion at 173 K, in the metastable absence of clathrate (from Mullis, 1976). The clathrate is nucleated at 123 K (arrows). At room temperature, a rim of liquid H₂O cannot be distinguished.

Molecules, such as CO_2 , CH_4 , N_2 , C_2H_6 , C_3H_8 (propane), C_4H_{10} (isobutane) may occupy the cavities. Molecules larger than n-butane do not fit in any type of cavity and are, therefore, unable to enter clathrate structures. CH_4 and CO_2 form preferentially *Structure-I* clathrates, and the N_2 *Structure-II* clathrates. C_3H_8 is able to form both clathrate structures at distinct conditions (Hafemann and Miller, 1969). Molecules larger than C_3H_8 may enter only in the larger cavities of *Structure-II* clathrates. *Structure-II* clathrate may coexist with *Structure-I* clathrate when the fluid inclusions contain mixtures of CO_2 , CH_4 and N_2 .

It is important noting that clathrates are non-stoichiometric compounds. If all cages are occupied, the ideal composition of *Structure-I* and *Structure-II* clathrates are:



where M denotes a gas molecule. The formula is normalised at one gas molecule. If only the larger cavities are filled, the composition of *Structure-I* and *Structure-II* clathrates are:



The variable stoichiometry seems to be temperature and pressure dependent, which resulted in large uncertainties of any direct chemical analysis.

The stability conditions of a clathrate is influenced by so-called inhibitors, like dissolved electrolytes and alcohols. These inhibitors do not enter clathrate structures, but lower the activity of the solute by means of affecting its fluid structure. Any concentration of dissolved electrolytes will lower the temperature of clathrate formation at a given pressure, similar to the effect of freezing-point-depression in gas-free solutions.

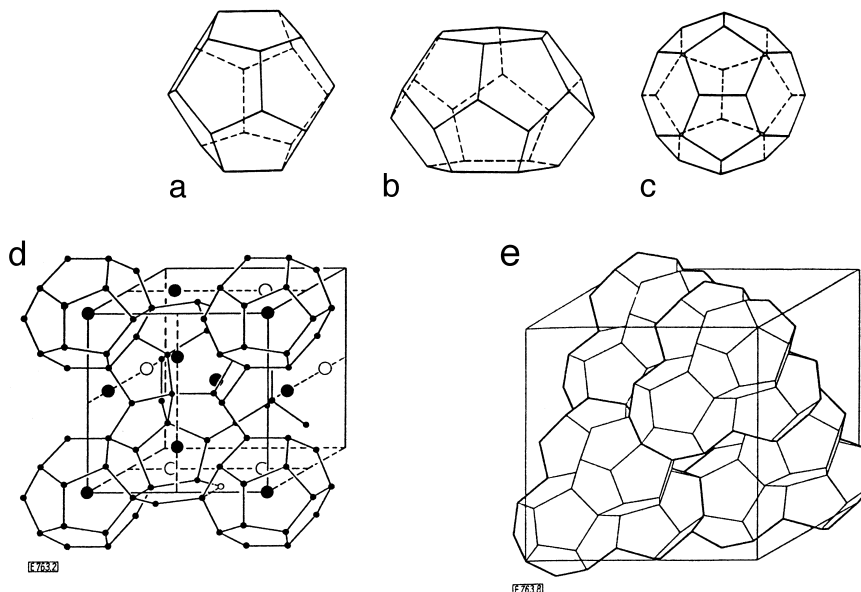
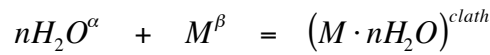


Fig.2. Three types of cavities within clathrate structures: pentagonal dodecahedron (a), tetrakaidecahedron (b), and hexakaidecahedron (c), which form the fundamental structural elements of Structure I clathrates (d) and Structure II clathrates (e). After Stackelberg and Müller (1954) and Sloan (1990).

Statistical model of clathrate stability conditions

Modifications of classical adsorption statistical mechanism, which include a three dimensional generalisation of ideal localised adsorption, were the first fundamental approaches to model clathrate stability (Waals and Platteeuw, 1959). The model assumes that a cavity may contain maximally one gas molecule, that no interaction exist between gas molecules, and that the engaged gas molecules are not distorting the host lattice. Characteristic aspects of this model were improved or adjusted by e.g. McKoy and Sinanoglu (1963), Parrish and Prausnitz (1972), Holder et al. (1980), Dharmawardhana et al. (1980), John et al. (1988), Munck et al. (1988), Dubessy et al. (1992) and Bakker et al. (in prep.).

The formation of a clathrate can be represented by an equilibrium reaction between three phases:



where M is a type of gas that is engaged, n is the amount of mole H₂O per mole engaged gas, α is an liquid aqueous solution or ice, and β is a vapour or a liquid phase. The chemical potential of each component must be equal for every phase in which that component is present at equilibrium conditions. Fractional filling of the cavities in the clathrate reduces the chemical potential of H₂O in this phase, thereby making it more stable:

$$\mu_{H_2O}^{clath} = \mu_{H_2O}^{empty} + RT \sum_i v_i \ln \left(1 - \sum_M y_{Mi} \right)$$

where $\mu_{H_2O}^{empty}$ is the chemical potential of a hypothetical empty clathrate, v_i is the number of cavities of type i per cage forming H₂O molecule, and y_{Mi} is the probability of finding a gas molecule M in a cavity of type i. The chemical potential of H₂O in the α phase is defined by:

$$\mu_{H_2O}^\alpha = \mu_{H_2O}^{pure} + RT \ln(a_{H_2O})$$

where a_{H_2O} is the activity of H₂O. In aqueous solutions, a_{H_2O} is affected by dissolved gases according to Henry's law (e.g. Wilhelm et al., 1977; Carroll et al. 1991) and electrolytes according to the product of the amount of dissolved ions and the osmotic coefficient (e.g. Debye and Hückel, 1923; Pitzer, 1992; Helgeson and Kirkham, 1974; Thurmond and Brass, 1988).

A relation was established between y_{Mi} and Langmuir-constants, according to the adsorption model of Waals and Platteeuw (1959):

$$y_{Mi}(T, P) = \frac{C_{Mi} f_M}{1 + \sum_K C_{Ki} f_K}$$

where C_{Mi} is the Langmuir-constant for gas M in a cavity of type i, and f_M is the fugacity of gas M. This equation is a generalised notation for mixed hydrates, which contain more than one engaged gas species (M and K). The Langmuir-constant is defined by molecular cell potentials within cavities:

$$C_{Mi}(T) = \frac{4\pi}{kT} \int_0^{\infty} \exp\left(\frac{-w(r)}{kT}\right) r^2 dr$$

where r is the distance to the centre of the cage, and $w(r)$ is the spherically symmetrical potential function describing the intermolecular potential between a gas molecule at the centre of a cage and a H_2O molecule in the cavity wall, which is average over all neighbouring H_2O molecules. The *Kihara-potential* (Kihara, 1953) which considers the size and shape of interacting molecules is used to calculate $w(r)$. This potential seems to give better predictions of dissociation pressures of clathrates at selected temperatures than the *Lennard-Jones 12-6 potential* (McKoy and Sinanoglu, 1963), as originally used by Waals and Platteeuw (1959).

An arbitrarily defined chemical potential difference $\Delta\mu$ between H_2O in the hypothetical empty clathrate and pure H_2O is used to obtain thermodynamic properties at any given temperature and pressure (Saito et al., 1964):

$$\frac{\Delta\mu(T,P)}{RT} = \frac{\mu_{H_2O}^{empty} - \mu_{H_2O}^{pure}}{RT} = \frac{\Delta\mu_0}{RT_0} - \int_{T_0}^T \frac{\Delta h}{RT^2} dT + \int_{P_0}^P \frac{\Delta v}{RT} dP$$

$$\Delta h(T) = \Delta h_0 + \int_{T_0}^T \Delta c_p dT$$

where Δh , Δv , and Δc_p are the enthalpy difference, molar volume difference, and heat capacity difference between an empty clathrate and pure H_2O , respectively. $\Delta\mu_0$ and Δh_0 are the chemical potential difference and the enthalpy difference at standard conditions. $\Delta\mu$ is considered a standard value for a given clathrate structure, because it is not related to the type of encaged gas molecule and dissolved substances in aqueous solutions.

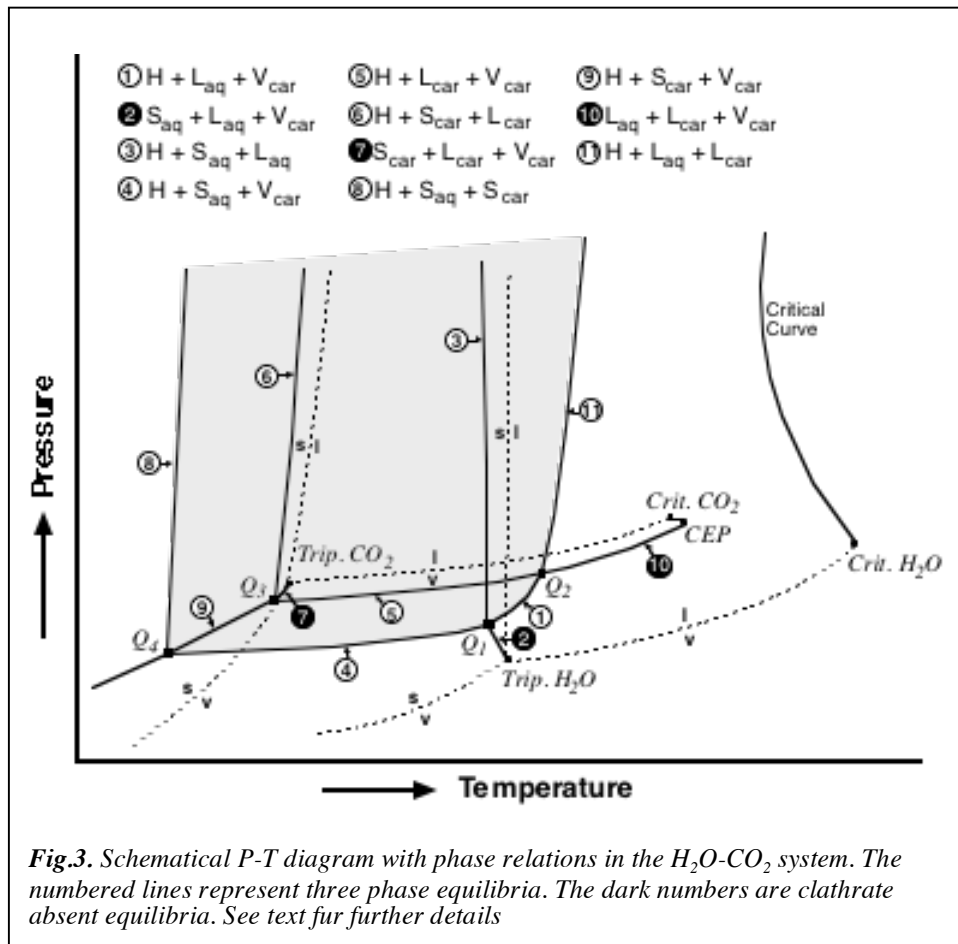
The accuracy and assumptions of this clathrate model were improved by the determination of more suitable *Kihara parameters* (e.g. Dubessy et al., 1992, Bakker et al., in prep.), according to the method of Parrish and Prausnitz (1972). Unknown *Kihara parameters* between a H_2O and a gas molecule in the clathrate structure were estimated with the least-square method, which compares experimental data points of clathrate dissociation conditions, i.e. temperature and pressure, to calculated values. The clathrate model can be used to calculate the stability conditions of clathrates containing any type of gas, in equilibrium with any type of aqueous solution. Furthermore, the model is able to calculate the stoichiometry of clathrates.

Symbols

H , S , L , and V stand for clathrate, solid, liquid and vapour phase, respectively. The subscripts *aq* and *car* denote aqueous and carbonic solution, where carbonic refers to any gas mixture of CO_2 , CH_4 , and N_2 .

Topology of the H₂O-CO₂ system

A pure qualitative P-T diagram of the binary system H₂O-CO₂ with schematically projected phase equilibria (Fig.3) illustrates the position of phase relations in perspective to the pure end-members. The univariant two-phase associations of pure H₂O and pure CO₂ are indicated with dashed lines: melting curve (*SL*), sublimation curve (*SV*), and boiling curve (*LV*). These lines intersect at invariant triple points, where vapour, liquid and solid coexist. The boiling curve ends at the invariant critical point, where the structural distinction between liquid and vapour vanishes. A thin line which connect critical points of different total compositions is projected into the diagram. This line is split into a low-temperature and a high temperature part (e.g. Heilig and Franck, 1989). The low temperature part of the critical curve starts from the pure CO₂ critical point, i.e. 304.2 K and 7.3858 MPa, and ends at a lower critical end point (*CEP*) at a slightly lower pressure and higher temperature. The high temperature part of the critical line starts from the H₂O critical point, i.e. 647.27 K and 22.12 MPa, shows a temperature minimum, and than runs to very high pressures as temperature increases. The thick solid lines illustrate the univariant three-phase associations in the binary H₂O-CO₂ system.



The maximum stability conditions of CO₂ clathrate are represented by the shaded area. The upper temperature limit of clathrate stability is line 11 (Fig.3), where it melts into unmixed

liquid-like fluids, a CO₂-rich and a H₂O-rich. At very low pressures, clathrate decomposes in a CO₂-rich vapour phase and ice or a H₂O-rich liquid solution (lines 4 and 1 in Fig.3, respectively). The lines intersect at invariant *quadruple points*: **Q1** (H+S_{aq}+L_{aq}+V_{car}), **Q2** (H+L_{aq}+L_{car}+V_{car}), **Q3** (H+S_{car}+L_{car}+V_{car}), and **Q4** (H+S_{aq}+S_{car}+V_{car}). The **Q4** point is hypothetically projected to illustrate a possible lower temperature limit of clathrate stability (line 8 in Fig.3), where it may unmix in solid CO₂ and ice.

In practice, projections as presented in Fig.3 may be confusing. For example, non-existent line-intersections may appear as a result of the projection method along composition, e.g. line 3 and 5. Line 3 occurs only for H₂O-rich fluid systems, up to about 13 mole% CO₂ (clathrate composition), while line 5 is valid for CO₂-richer fluids. The amount of dissolved components or composition of each phase is not revealed in Fig.3, which may, however, control the characteristic phase changes. The quadruple point **Q3** is not present in H₂O-rich fluids, and, consequently, line 5, 6, and 9 do not occur. The critical point of CO₂ is very close to *CEP* and can hardly be distinguished. Consequently, the three-phase L_{aq}+L_{car}+V_{car} (line 10) and its extension H+L_{car}+V_{car} (line 5) coincide with the boiling curve of pure CO₂. Furthermore, two distinct temperature and pressure values were estimated for the position of **Q1**: 271.67 K and 1.04 MPa according to Larson (1955) and Bozzo et al. (1975), and 273.15 K and 1.26 MPa according to Davidson (1973) and Sloan (1990). Systematic **Q1** values at 273.15 K would cause a coincide of the melting curve of pure H₂O and line 2 and 3 (Fig.3). Within synthetic H₂O-CO₂-rich fluid inclusions **Q1** is determined at 271.7 K (pers. comm. M. Dubois).

The actual phase relations in the H₂O-CO₂ system are revealed in Fig.4. To characterise all phase equilibria in this system, a P-T diagram is constructed for a fluid which is CO₂-richer than the clathrate phase (Fig.4a) and which is CO₂-poorer than the clathrate phase (Fig.4b). These two projections do not display any non-existent intersections.

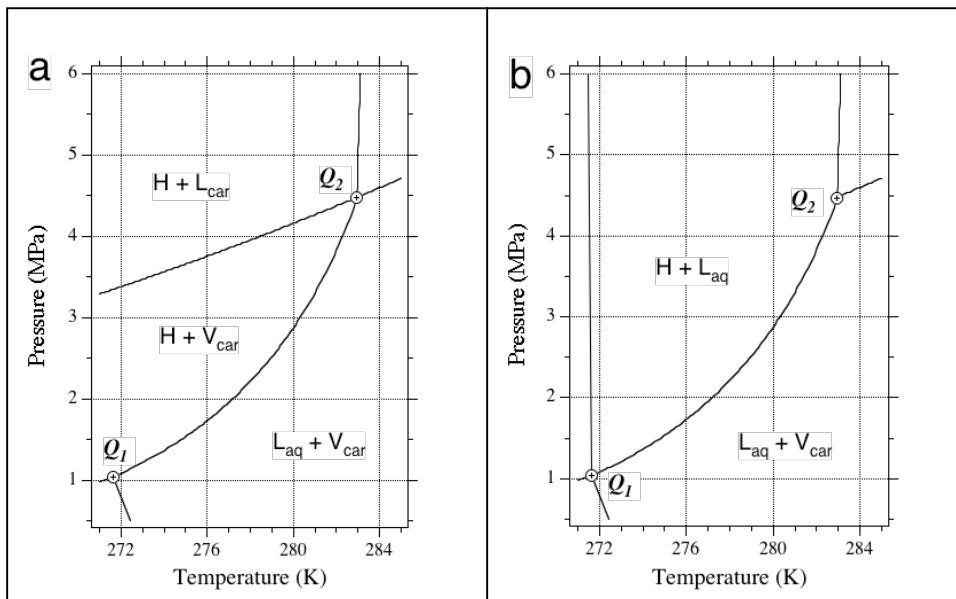


Fig.4. P-T diagrams with actual stability conditions of CO₂-clathrate for CO₂-rich fluids (a) and H₂O-rich fluids (b). See text for further details.

Several semi-schematic isobaric T-X diagrams (Fig.5) are constructed over a wide range of selected pressures to elucidate any misinterpretation of Fig.3. Fig.5 is based on experimental data of the solvus (Tödheide and Franck, 1963; Takenouchi and Kennedy, 1964; Sterner and Bodnar, 1991), mutual solubility (e.g. Wilhelm et al., 1977; Carroll et al., 1991; Carroll and Mather, 1992), and clathrate stability (Deaton and Frost, 1946; Unruh and Katz, 1949; Larson, 1955; Robinson and Metha, 1971). The P-T conditions of univariant and invariant phase transitions of the pure end members are obtained from Bridgeman and Aldrich (1964) and Vargaftic (1975) for H₂O, and Angus et al. (1976) and Duschek et al. (1990) for CO₂. The diagrams are not drawn to scale, as solubilities are very small. Some parts have been greatly over-emphasised, as they are important for the understanding of phase relations. The composition of the clathrate is taken as nearly constant to a first approximation.

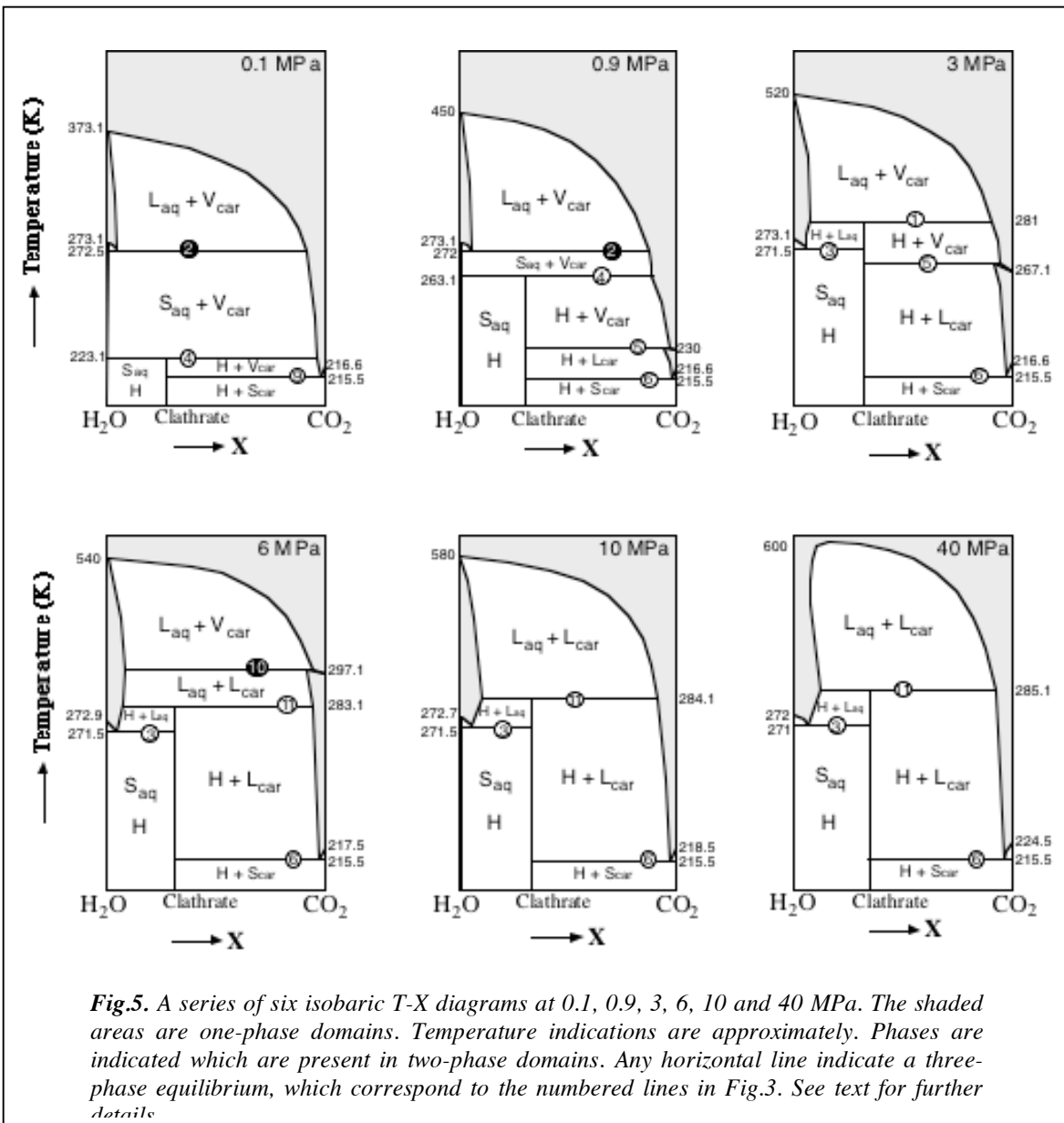


Fig.5. A series of six isobaric T-X diagrams at 0.1, 0.9, 3, 6, 10 and 40 MPa. The shaded areas are one-phase domains. Temperature indications are approximately. Phases are indicated which are present in two-phase domains. Any horizontal line indicate a three-phase equilibrium, which correspond to the numbered lines in Fig.3. See text for further details

At room pressure (0.1 MPa), the clathrate is occurring at very low temperatures, below 223.1 K. Liquid-like CO₂ is not present at this relatively low pressure condition, which is below the triple point of pure CO₂, 216.58 K and 0.5185 MPa. At higher temperatures, a CO₂-rich vapour is in equilibrium with pure ice, and above 272.5 K with a H₂O-rich liquid. At 0.9 MPa, near **Q1** pressure, the clathrate stability field has expanded to 263.1 K. Liquid-like CO₂ appears at lower temperatures, between 215.5 and 230 K, and vapour-like CO₂ above these temperatures. At 3 MPa between **Q1** and **Q2** pressures, clathrate is occurring at still higher temperatures (281 K), however the temperature dependence decreases steadily. Clathrate may occur in the absent of ice. The CO₂-rich liquid monophasic domain has expanded to 267.1 K. At 6 MPa above **Q2** pressure, the transition of a CO₂-rich liquid to a CO₂-rich vapour occurs at higher temperatures (297.1 K) than the melting temperature of clathrate (283.1 K). At 10 MPa, above the critical pressure of pure CO₂, monophasic domains of both CO₂-rich liquid and vapour are joined and the structure of this supercritical CO₂-rich fluid resembles a liquid phase. The most pronounced alteration between 10 and 40 MPa is the change of CO₂ solubility in liquid H₂O. which decreases at higher temperatures at 10 MPa, but increases at 40 MPa. As a result, the separated one-phase domains of a H₂O-rich liquid and a CO₂-richer vapour are united and the immiscibility domain detaches from the pure H₂O axis.

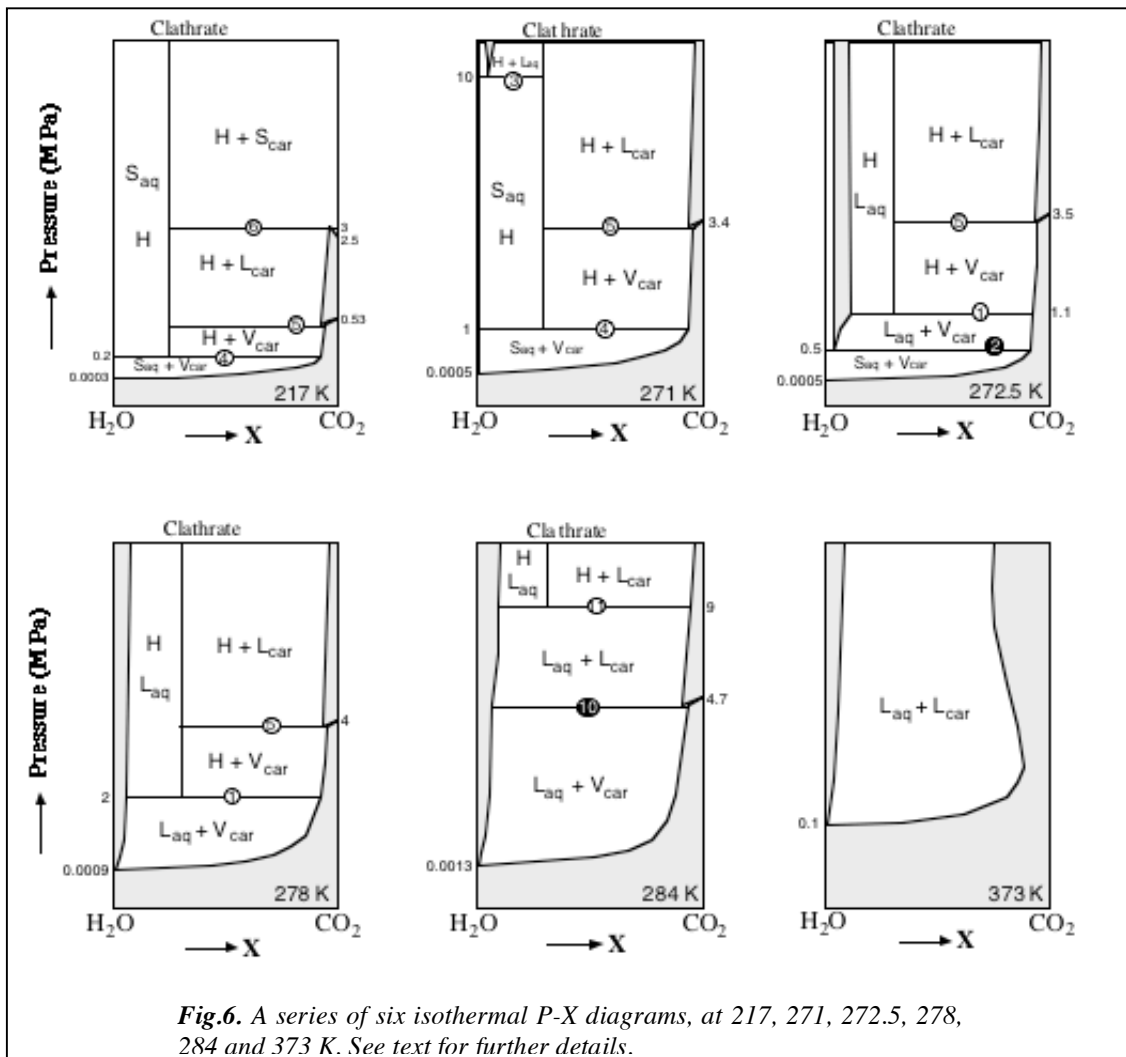
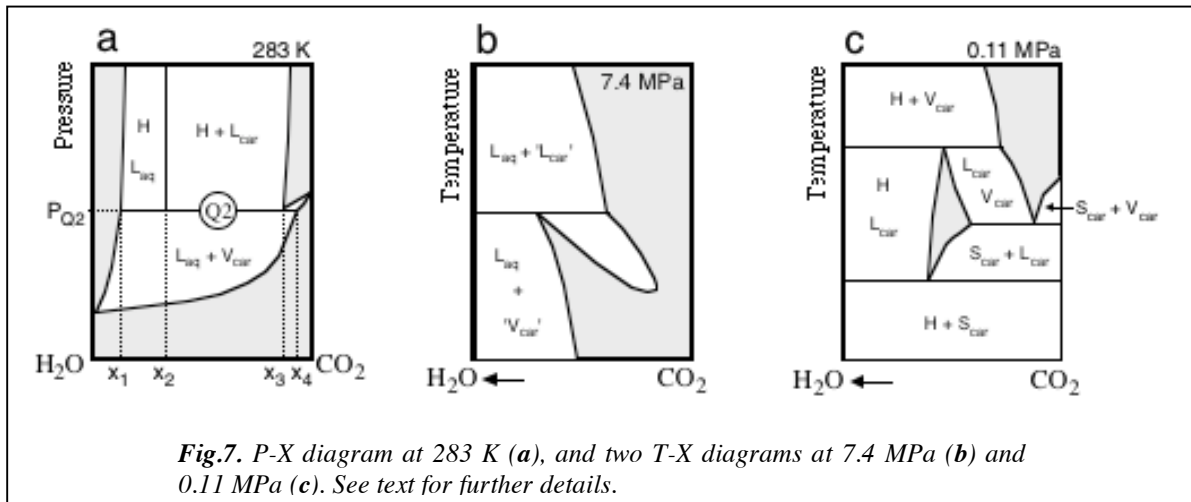


Fig.6. A series of six isothermal P-X diagrams, at 217, 271, 272.5, 278, 284 and 373 K. See text for further details.

In addition, several isothermal P-X sections are shown in Fig.6, with increasing temperatures. Similar to the T-X diagrams (Fig.5) these diagrams are not drawn to scale, and the indicated pressures are approximate. The diagrams in Fig.6 may change drastically within very small temperature intervals because several phase transitions are nearly pressure independent (lines 3, 6, 8, and 11 in Fig.3). Diagrams are not constructed for temperatures below the triple point of pure CO₂, because P-T conditions for **Q3** and **Q4** are unknown. Similar phase transitions as in Fig.5 are illustrated from a different perspective. At 373 K, L_{aq}+V_{car} domain is the only remaining immiscibility region. The supercritical CO₂-rich phase resembles a vapour at low pressures and gradually changes to a liquid-like fluid at higher pressures.

Fig.7 focuses on three characteristic occurrences of Fig.5 and 6. **Q2** conditions are intersected between 278 and 284 K in Fig.6. The H+L_{aq}+L_{car} curve (line 11 in Fig.3) is more sensitive to temperature changes than the L_{aq}+L_{car}+V_{car} curve (line 10 in Fig.3), and consequently, they coincide at **Q2** conditions (Fig.7a), where clathrate (x₂) is stable with a H₂O-rich liquid of composition x₁, a CO₂-rich liquid of composition x₃, and a CO₂-rich vapour of composition x₄. Fig.7b illustrates the theoretical occurrence of a critical point in a CO₂-rich fluid system between the critical pressure of pure CO₂ and the *CEP*. A very small domain of coexisting CO₂-rich liquid and vapour is present. The coexistence of a CO₂-rich solid, liquid and vapour with very small amounts of dissolved H₂O is illustrated in Fig.7c (line 7 in Fig.3). This figure also illustrate the extremely small freezing point depression of the pure CO₂ triple point if H₂O is added to the system.



Topology of the H₂O-CH₄ system

The H₂O-CH₄ fluid system (Fig.8) as described by Kobayashi and Katz (1949), displays a different phase transition behaviour than the H₂O-CO₂ system. The differences are mainly induced by the relatively low critical point of pure CH₄, 190.55 K and 4.595 MPa, which is located within the clathrate stability field. Consequently, the invariant point **Q2** is not present in

this system, and the $H+L_{aq}+V_{car}$ curve (line 1 in Fig.8) extends to extreme high pressures. Furthermore, the pure CH_4 boiling curve occurs at slightly lower pressure than the $H+L_{car}+V_{car}$ (line 5 in Fig.8), and the *CEP* lies above the critical point of pure CH_4 .

Three T-X diagrams (Fig.9) are constructed to indicate the similarities between the H_2O-CO_2 system and the H_2O-CH_4 system. The thermodynamic data for pure CH_4 are obtained from Angus et al. (1978). At 0.01 MPa, the CH_4 clathrate occurs at very low temperatures, similar to the H_2O-CO_2 system. At pressures above 4.595 MPa, the two phase domain of CH_4 -rich liquid and CH_4 -rich vapour disappears at temperatures below the dissociation temperature of clathrate. At higher pressures, this system is again very similar to the H_2O-CO_2 system above the critical conditions for pure CO_2 .

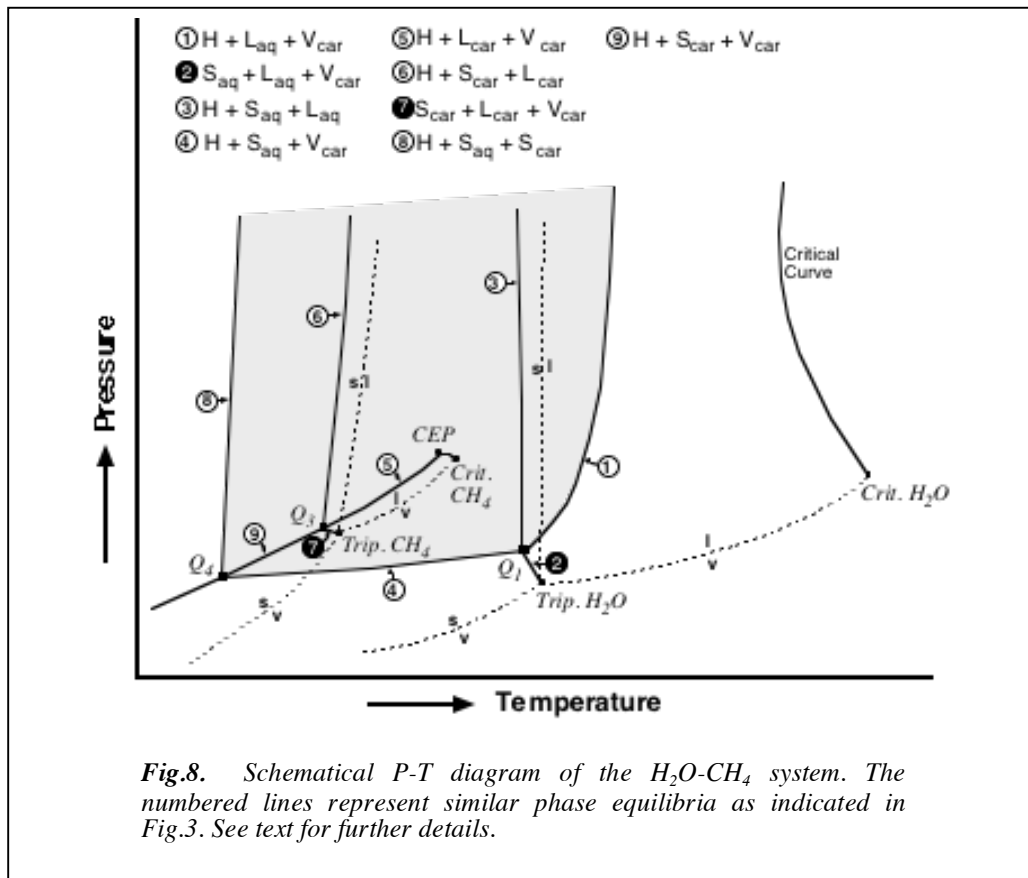
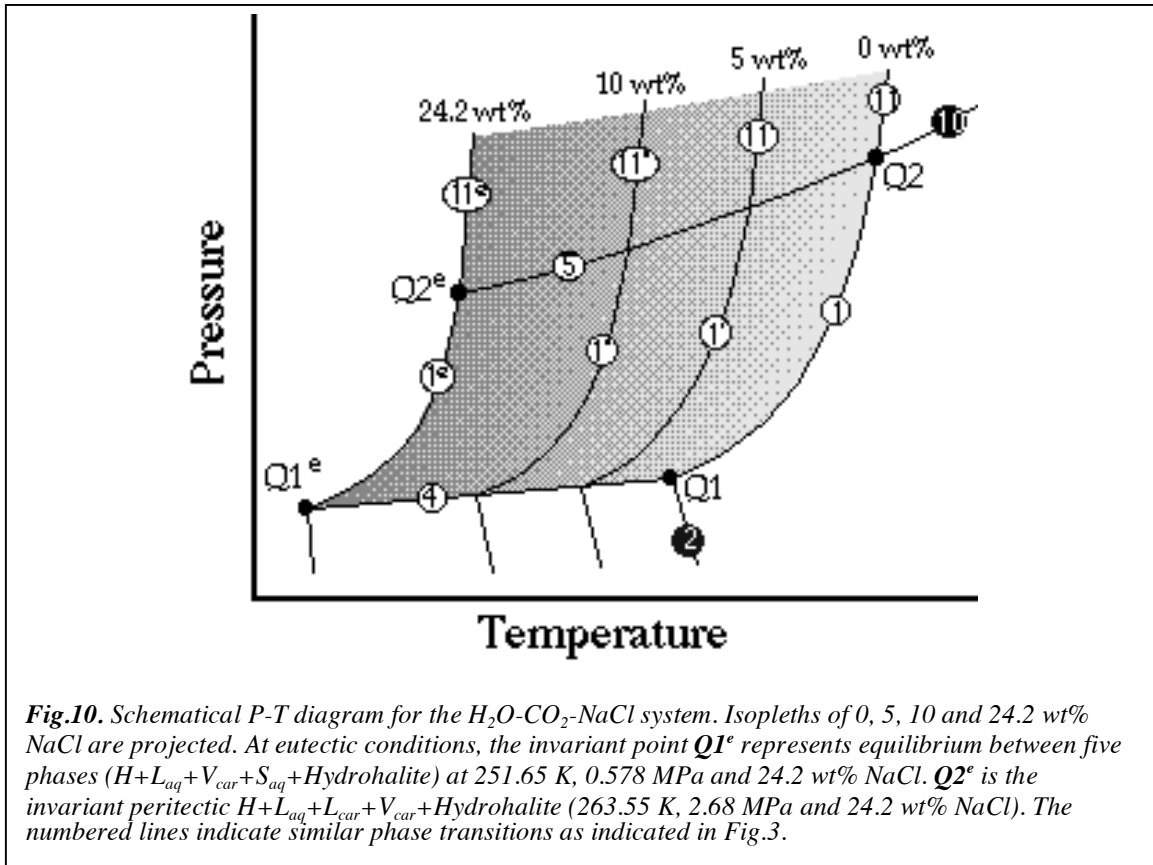
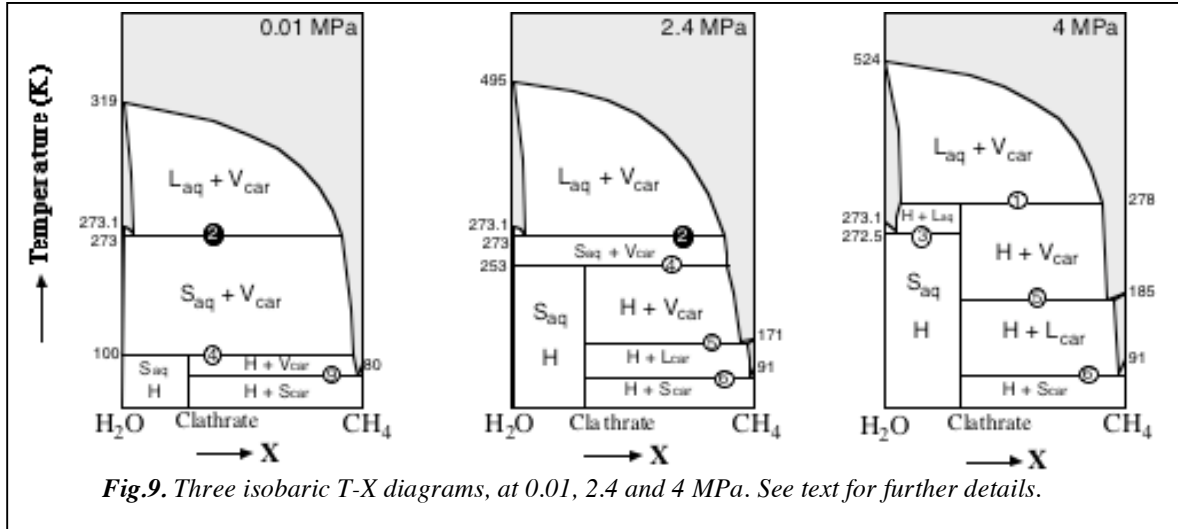


Fig.8. Schematic P-T diagram of the H_2O-CH_4 system. The numbered lines represent similar phase equilibria as indicated in Fig.3. See text for further details.

Topology of the H_2O-CO_2-NaCl system

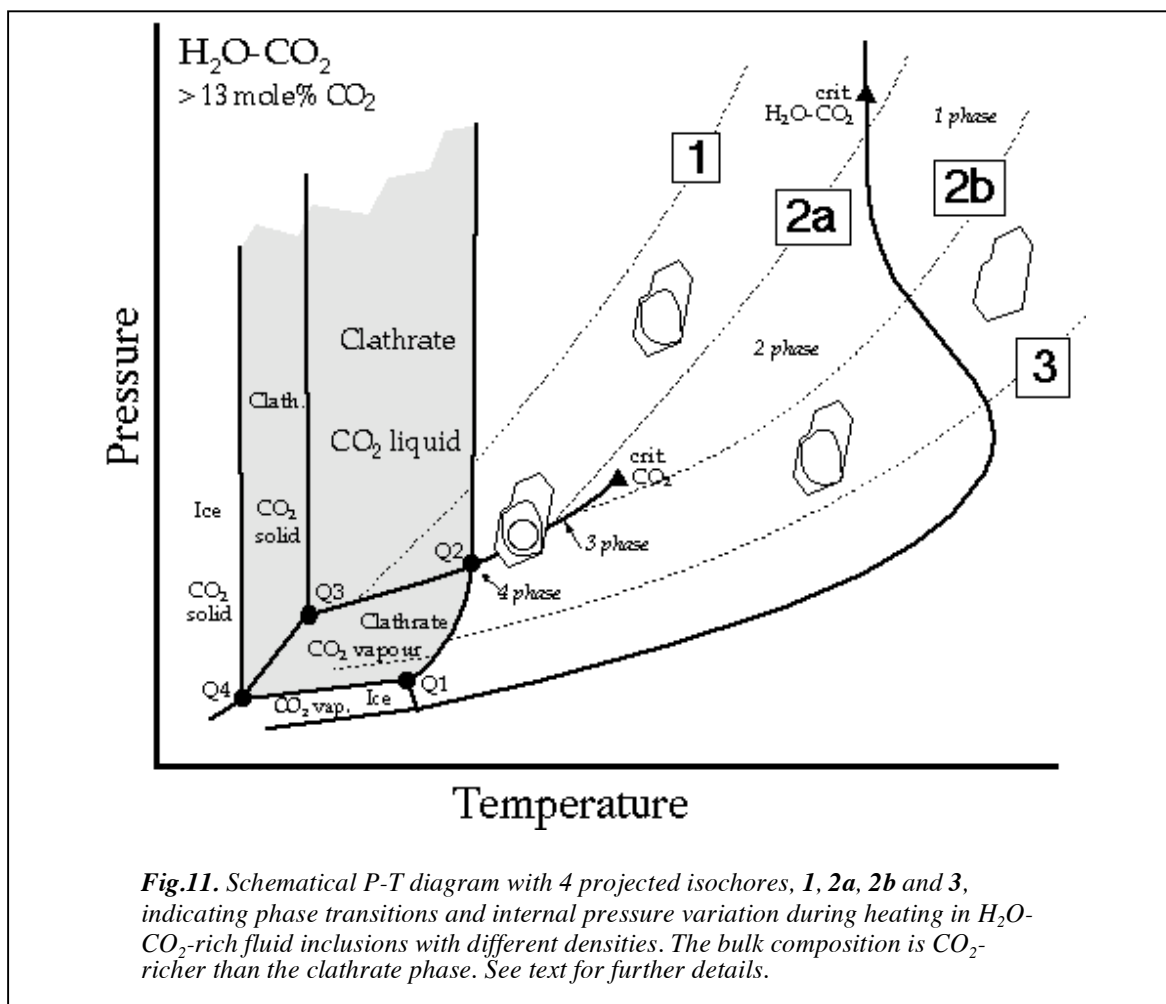
The addition of NaCl to the H_2O-CO_2 system increases the variance of the system, and decreases the ability to illustrate phase transitions within two-dimensional graphs, where univariant curves represent equilibria between four phases, and 5 coexisting phases are displayed by invariant points. The presence of clathrate in this ternary system was experimentally investigated by Larson (1955), Bozzo et al. (1975), and Diamond (1992). Darling (1991) improved the empirical equation for the temperature depression of Q_2 melting behaviour as a function of salinity from Bozzo et al. (1975). Barton and Chou (1993) calculated the liquidus for the H_2O -rich corner of this system. The stability field of CO_2 -clathrate is

reduced by any type of additional salt (Fig.10), as the $H+L_{aq}+V_{car}$ curve (line 1), $S_{aq}+L_{aq}+V_{car}$ curve (line 2) and $H+L_{aq}+L_{car}$ curve (line 11) are shifted towards lower temperatures with increasing salinities, similar to the effect of freezing point depression. These curve will shift back again to higher temperatures for fluids which are more saline than the eutectic point, 24.2 wt% NaCl.



Clathrates in fluid inclusions

During phase transition analysis of fluid inclusions using a heating-freezing stage, inclusions are assumed to have a constant absolute volume. Decrepitation is easily detected and shrinkage or expansion of the host crystal is neglected. Therefore, fluid inclusions are isochoric systems. Projected phase transitions in V-X diagrams at selected temperatures may clearly indicate the evolution of the entrapped fluid during a heating sequence. The formation of solid phases in fluid inclusions changes the density and molar volume of the fluid, and corresponding pressures have to be obtained to calculate the molar volume of each phase present. A P-T diagram is constructed for the H₂O-CO₂ system (Fig.11) to illustrate isochoric cuttings.



Phase transitions in fluid inclusions along these isochores are schematically drawn in Fig.12. Isochore 1 represent a relative high total density fluid with a liquid-like CO₂ phase. At temperatures below Q₃ along curve 9 (Fig.3) fluid inclusions contain two solid phases, i.e. clathrate and solid CO₂, and a CO₂-rich vapour. At Q₃, the CO₂ melts and a bubble appears with a clear meniscus, marking the boundary between liquid and vapour CO₂. These phases homogenise to the liquid phase before the clathrate is melted, and the system moves into a two phase domain.

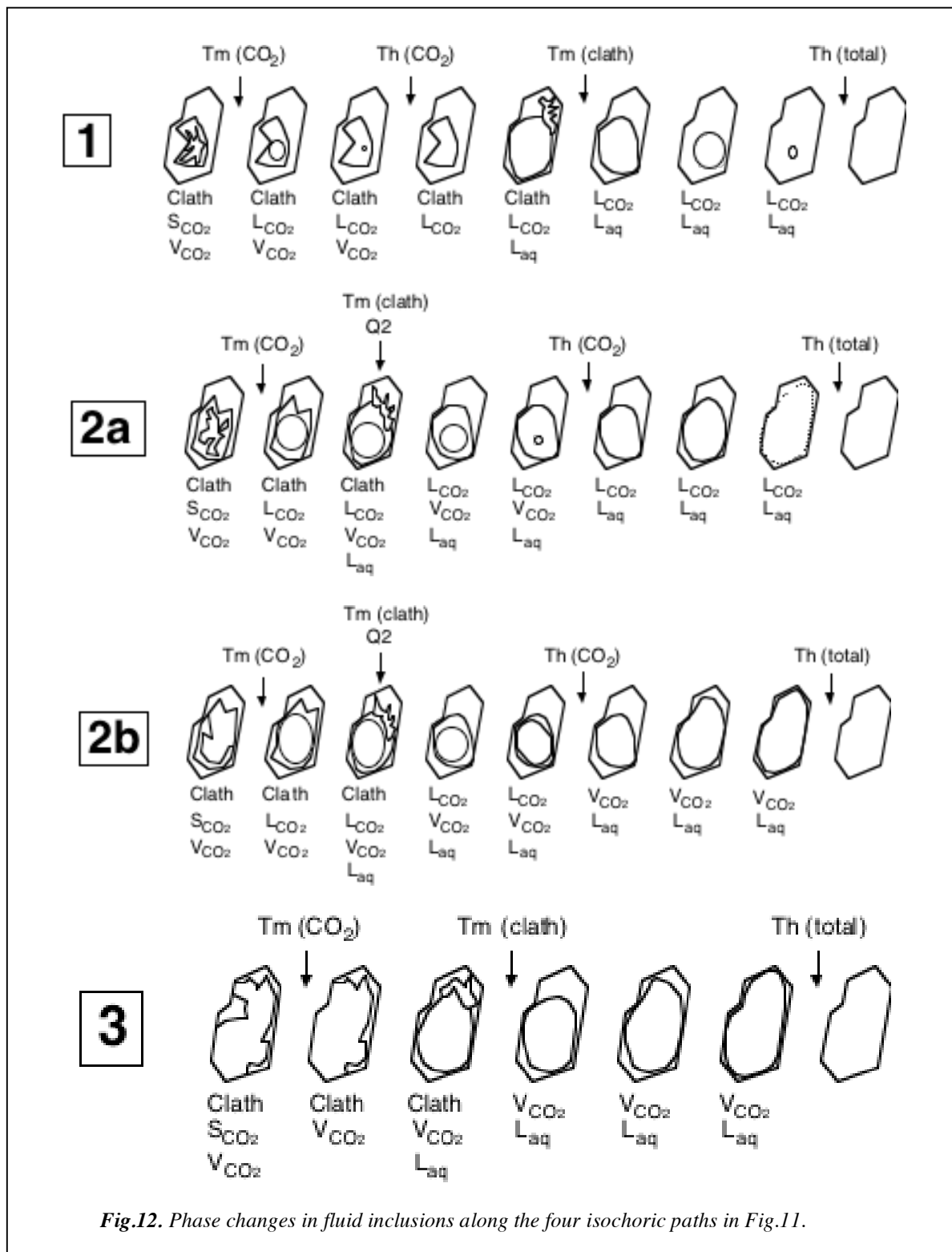


Fig.12. Phase changes in fluid inclusions along the four isochoric paths in Fig.11.

At the intersection with curve 11 clathrate start to melt, releasing free liquid H₂O and CO₂, which increases the density of the CO₂ phase. During a melt trajectory, the system shifts to a higher density isochore until all the clathrate is melted. The two remain phases, i.e. CO₂-rich liquid and H₂O-rich liquid homogenise at higher temperatures and extreme high pressures. Towards this homogenisation, the solubility of H₂O in the CO₂ phase increases and the isochore from the two phase fluid bends steadily towards the final isochore of the complete homogeneous fluid. At lower CO₂ densities, isochore **2a** (Fig.12) illustrates a fluid system which shows clathrate melting at **Q2** conditions before homogenisation of the CO₂ phases. The pressure evolves along the boiling curve of CO₂ (line 5 in Fig.3) during heating, because both CO₂ liquid and vapour remain present.. Although, homogenisation of the CO₂ occurs in the liquid phase, the total homogenisation occurs in the vapour phase, because the critical point for this particular fluid composition is located at higher pressure. Isochore **2b** illustrate a similar fluid system, where the CO₂ phases homogenise in the vapour phase. Further phase changes are similar to isochore **2a**. Fluid inclusions with a very low CO₂ density contain a mixture of clathrate and a CO₂-rich vapour, isochore 3 (Fig.12). These inclusions have a much larger clathrate melting trajectory , because the curved stability boundary (line 1 in Fig.3) indicate an increased temperature sensitivity for equal pressure intervals. In special cases, CO₂ densities may reach **Q2** conditions during clathrate melting, which illustrates a phase separation during a heating run.

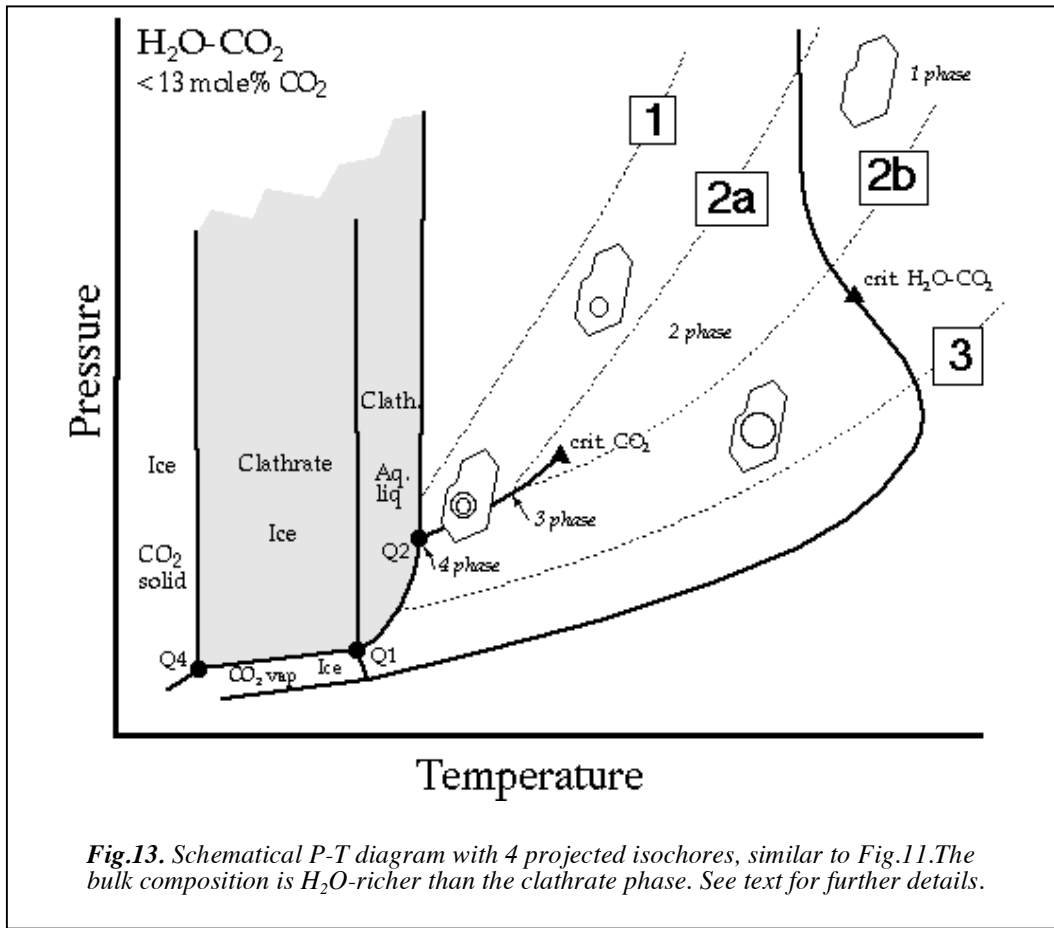


Fig.13. Schematic P-T diagram with 4 projected isochores, similar to Fig.11. The bulk composition is H₂O-richer than the clathrate phase. See text for further details.

Fluids which are richer in H₂O than the composition of the clathrate phase (Fig.13) do not in general enter the clathrate stability field. Outside this field, the isochoric sections drawn in Fig.13 represent similar phase changes as shown in Fig.12. At low temperatures, the inclusions contain a mixture of clathrate, ice and a very low density CO₂-rich vapour (line 4 in Fig.3), because most of the CO₂ is absorbed in the clathrate phase. The ice melts completely at **Q1** conditions, and a bubble appears which marks the boundary between an aqueous liquid solution and a CO₂-rich vapour in the presence of a solid clathrate phase. During further heating, the pressure inside the inclusion increases due to the release of CO₂ from the melting clathrate phase, and the fluid system moves towards **Q2** along curve 1. A combination of the final ice melting temperature and the final clathrate melting temperature was used by Dubessy et al. (1992) and Yerokin(1993) to calculate the bulk salinity of fluid inclusions. The final ice melting temperature cannot be used for salinity estimations because the melting clathrate will further dilute the solution. These calculation also depends on estimations of volume fractions of the phases present in inclusions after clathrate melting, and, consequently, the bulk composition and density may be calculated.

Acknowledgements

This work has been supported by the program 'Human Capital and Mobility' from the CEC (network HCM, CEE-XII G - contract CT 930198 - PL 922279): Hydrothermal/Metamorphic water rock interactions in crystalline rocks: a multidisciplinary approach based on paleofluid analysis. We thank J. Dubessy for constructive comments.

References

- ANGUS, S., ARMSTRONG, B. & DE REUCK, K. M. 1976. *International thermodynamic tables of the fluid state: 3. Carbon Dioxide*. Pergamon Press, Oxford.
- ANGUS, S., ARMSTRONG, B. & DE REUCK, K. M. 1978. *International thermodynamic tables of the fluid state: 5. Methane*. Pergamon Press, Oxford.
- BAKKER, R. J., DUBESSY, J. & CATHELINEAU, M. *in prep*. Improvements in clathrate modelling I: The H₂O-CO₂ system with various salts. *Geochimica et Cosmochimica Acta*.
- BARTON, P.B. & CHOU I. MING 1993. Calculation of the vapor-saturated liquidus for the NaCl-CO₂-H₂O system. *Geochimica et Cosmochimica Acta*, **57**, 2715-2723.
- BODNAR, R.J. 1983. A method of calculating fluid inclusion volumes based on vapor bubble diameters and P-V-T-X properties of inclusion fluids. *Economic Geology*, **78**, 535-542.
- BOZZO, A. T., CHEN, H.-S., KASS, J. R. & BARDUHN, A. J. 1975. The properties of the hydrates of chlorine and carbon dioxide. *Desalination*, **16**, 303-320.
- BRIDGEMAN, O.C. & ALDRICH, E.W. 1964. Vapor pressure tables for water. *Journal of Heat Transfer*, **86C**, 279-286.
- CARROLL, J. J. & MATHER, A. E. 1992. The system carbon dioxide-water and the Krichevsky-Kasarnovsky equation. *Journal of Solution Chemistry*, **21**, 607-621.
- CARROLL, J. J., SLUPSKY, J. D. & MATHER, A. E. 1991. The solubility of carbon dioxide in water at low pressure: *Journal of Physical Chemistry Reference Data*, **20**, 1201-1209.
- DARLING, R.S. 1991. An extended equation to calculate NaCl contents from final clathrate melting temperatures in H₂O-CO₂-NaCl fluid inclusions: Implications for P-T isochore location. *Geochimica et Cosmochimica Acta*, **55**, 3869-3871.
- DAVIDSON, D.W. 1973. *Clathrate hydrates*. In: Franks F. (ed.) Water in crystalline hydrates; Aqueous solutions of simple nonelectrolytes. Plenum Press, **2**, 115-234.

- DEATON, W. M. & FROST, E. M. jr. 1946. *Gas hydrates and their relation to operation of natural-gas pipe lines*. United States Bureau of Minerals Monograph, **8**, 1-108.
- DEBYE, P. & HÜCKEL, E. 1923. Zur Theorie der Electrolyte I: Gefrierpunktserniedrigung und verwandte Erscheinungen. *Physikalisch Zeitschrift*, **24**, 185-206.
- DHARMAWARDHAMA, P. B., PARRISH, W. R. & SLOAN, E. D. jr. 1980. Experimental thermodynamic parameters for the prediction of natural gas hydrate dissociation conditions. *Industrial Engineering and Chemical Fundamentals*, **19**, 410-414.
- DIAMOND, L.W. 1992. Stability of CO₂ clathrate hydrate + CO₂ liquid + CO₂ vapour + aqueous KCl-NaCl solutions: Experimental determination and application to salinity estimates of fluid inclusions. *Geochimica et Cosmochimica Acta*, **56**, 273-280.
- DIAMOND, L.W. 1994. Salinity of multivolatiles fluid inclusions determined from clathrate hydrate stability. *Geochimica et Cosmochimica Acta*, **58**, 19-41.
- DUBESSY, J., THIÉRY, R. & CANALS, M. 1992. Modelling of phase equilibria involving mixed gas clathrates: application to the determination of molar volume of the vapour phase and salinity of aqueous solution in fluid inclusions. *European Journal of Mineralogy*, **4**, 873-884.
- DUSCHEK, W., KLEINRAHM, R. & WAGNER, W. 1990. Measurement and correlation of the (pressure, density, temperature) relation of carbon dioxide II: Saturated-liquid and saturated-vapour densities and the vapour pressure along the entire coexistence curve. *Journal of Chemical Thermodynamics*, **22**, 841-864.
- HAFEMANN, D.R. & MILLER, S.L. 1969. The clathrate hydrates of cyclopropane. *Journal of Physical Chemistry*, **73**, 1392-1397.
- HEILIG, M. & FRANCK, E.U. 1989. Calculation of thermodynamic properties of binary fluid mixtures to high temperatures and pressures. *Berichte der Bunsengesellschaft für Physikalische Chemie*, **93**, 898-905.
- HELGESON, H.C. & KIRKHAM, D.H. 1974. Theoretical prediction of the thermodynamic behavior of aqueous electrolytes at high pressures and temperatures: I: Summary of the thermodynamic/electrostatic properties of the solvent. *American Journal of Science*, **274**, 1089-1198.
- HOLDER, G. D., CORBIN, G. & PAPADOPOULOS, K. D. 1980. Thermodynamic and molecular properties of gas hydrates from mixtures containing methane, argon, and krypton. *Industrial Engineering and Chemistry Fundamentals*, **19**, 282-286.
- JOHN, V. T., PAPADOPOULOS, K. D. & HOLDER, G. D. 1985. A generalized model for predicting equilibrium conditions for gas hydrates. *American Institute of Chemical Engineering Journal*, **31**, 252-259.
- KIHARA, T. 1953. Virial coefficients and models of molecules in gases. *Reviews in Modern Physics*, **25**, 831-843.
- KOBAYASHI, R. & KATZ, D. L. 1949. Methane hydrate at high pressures. *Petroleum Transactions, American Institute for Mechanical Engineers*, 66-70.
- LARSON, S. D. 1955. *Phase studies of two-component carbon dioxide-water system involving the carbon dioxide hydrate*. PhD Thesis, University of Illinois.
- MCKOY, V. & SINANOGLU, O. 1963. Theory of dissociation pressures of some gas hydrates. *Journal of Chemical Physics*, **38**, 2946-2956.
- MUNCK, J., SKJOLD-JORGENSEN, S. & RASMUSSEN, P. 1988. Computations of the formation of gas hydrates. *Chemical Engineering Data*, **27**, 22-24.
- MULLIS, J. 1976. Das Wachstumsmilieu der Quarzkristalle im Val d'Illeiez (Wallis, Schweiz). *Schweizerische mineralogische und petrographische Mitteilungen*, **56**, 219-268.
- PARRISH, W. R. & PRAUSNITZ, J. M. 1972. Dissociation pressure of gas hydrates formed by gas mixtures. *Industrial and Engineering Chemistry, Processes, Design, and Development*, **11**, 26-35.
- PITZER, K. S. 1992. Ion interaction approach: theory and data correlation. In: Pitzer, K. S. (ed) *Activity Coefficient in Electrolyte Solutions*. CRC Press, Boca Raton, Florida, 76-153.
- POTTER, R.W. II & BROWN, D.L. 1977. The volumetric properties of aqueous sodium chloride solutions from 0° to 500°C at pressures up to 2000 bars based on a regression of available data in the literature. *U.S. Geological Survey Bulletin*, **1421-C**, 36p.
- PRAUSNITZ, J. M., LICHTENTHALER, R. N. & DE AZEVEDO, E.G. 1986. *Molecular thermodynamics of fluid-phase equilibria*. Prentice Hall Inc., Englewood Cliffs, New Jersey.
- ROBINSON, D. B. & METHA, B. R. 1971. Hydrates in the propane-carbon dioxide-water system. *Journal of Canadian Petroleum Technology*, **10**, 33-35.
- SAITO, S., MARSHALL, D. R. & KOBAYASHI, R. 1964. Hydrates at high pressures, part II: Application of statistical mechanics to the study of the hydrates of methane, argon, and nitrogen. *American Institute of Chemical Engineering Journal*, **10**, 734-740.
- SLOAN, E.D. jr. 1990. *Clathrate Hydrates of Natural Gases*, Chemical Industries **39**, Marcel Dekker Inc.

- STERNER, S.M. & BODNAR, R.J. 1991. Synthetic fluid inclusions. X: Experimental determination of P-V-T-X properties in the CO₂-H₂O system to 6 kb and 700 °C. *American Journal of Science*, **291**, 1-54.
- TAKENOUCI, S. & KENNEDY, G. C. 1965. Dissociation of the phase CO₂-5.75H₂O. *Journal of Geology*, **73**, 383-390.
- THIÉRY, R., VIDAL, J. & DUBESSY, J. 1994. Phase equilibria modelling applied to fluid inclusions: Liquid-vapour equilibria and calculations of the molar volume in the CO₂-CH₄-N₂ system. *Geochimica et Cosmochimica Acta*, **58**, 1073-1082.
- THURMOND, V.L. & BRASS, G.W. 1988. Activity and osmotic coefficients of NaCl in concentrated solutions from 0 to -40°C. *Journal of Chemistry and Engineering Data*, **33**, 411-414.
- TÖDHEIDE, K. & FRANCK, E.U. 1963. Das Zweiphasengebiet und die kritische Kurve im System Kohlendioxid-Wasser bis zu Drucken von 3,5000 bar. *Zeitschrift für Physikalische Chemie Neue Folge*, **37**, 387-401.
- UNRUH, C. H. & KATZ, D. L. 1949. Gas hydrates of carbon dioxide-methane mixtures. *Journal of Petroleum Technology*, **1**, 83-86.
- VAN DEN KERKHOFF, A.M. 1990. Isochoric phase diagrams in the systems CO₂-CH₄ and CO₂-N₂: Application to fluid inclusions. *Geochimica et Cosmochimica Acta*, **54**, 621-629.
- VAN DER WAALS, J. H. & PLATTEEUW, J. C. 1959. Clathrate solutions. *Advances in Chemical Physics*, **2**, 1-57.
- VARGAFTIC, N.B. 1975. *Tables on the thermophysical properties of liquids and gases, in normal and dissociated states*. John Wiley and Sons, 739 p.
- VON STACKELBERG, M. & MÜLLER, H. R. (1954) Feste Gashydrate II: Struktur und Raumchemie. *Zeitschrift für Electrochemie*, **58**, 25-39.
- WILHELM, E., BATTINO, R. & WILCOCK, R.J. 1977. Low pressure solubility of gasses in liquid water. *Chemical Reviews*, **77**, 219-262.
- YEROKHIN, A.M. 1993. A new method of determining CO₂ density and solution concentration in H₂O-CO₂-NaCl inclusions from the gas-hydrate melting point. *Geochemistry International*, **30**, 107-129.